



Aged keratinocyte phenotyping: Morphology, biochemical markers and effects of Dead Sea minerals

Yoram Soroka^a, Zeev Ma'or^{a,b}, Yael Leshem^{a,b}, Lilian Verochovsky^a, Rami Neuman^c, François Menahem Brégégère^a, Yoram Milner^{a,*}

^aMyers Laboratory of Skin Biology and Biochemistry, Department of Biological Chemistry, The Hebrew University of Jerusalem at Givat Ram, Jerusalem 91904, Israel

^bDead Sea and Arava Science Center, Dead Sea, Israel

^cDepartment of Cosmetic Surgery, Hadassa Hospital Ein Karem, Jerusalem, Israel

ARTICLE INFO

Article history:

Received 9 December 2007

Received in revised form 4 August 2008

Accepted 5 August 2008

Available online 12 August 2008

Keywords:

Skin aging markers
Photodamage
Keratinocyte senescence
Dead Sea minerals
Biomarker profiling

ABSTRACT

The aging process and its characterization in keratinocytes have not been studied in depth until now. We have assessed the cellular and molecular characteristics of aged epidermal keratinocytes in monolayer cultures and in skin by measuring their morphological, fluorometric and biochemical properties. Light and electron microscopy, as well as flow cytometry, revealed increase in cell size, changes in cell shape, alterations in mitochondrial structure and cytoplasmic content with aging. We showed that the expression of 16 biochemical markers was altered in aged cultured cells and in tissues, including caspases 1 and 3 and β -galactosidase activities, immunoreactivities of p16, Ki67, 20S proteasome and effectors of the Fas-dependent apoptotic pathway. Aged cells diversity, and individual variability of aging markers, call for a multifunctional assessment of the aging phenomenon, and of its modulation by drugs. As a test case, we have measured the effects of Dead Sea minerals on keratinocyte cultures and human skin, and found that they stimulate proliferation and mitochondrial activity, decrease the expression of some aging markers, and limit apoptotic damage after UVB irradiation.

© 2008 Published by Elsevier Inc.

1. Introduction

Replicative senescence is characterized by the limited replicative lifespan of cells in culture (Hayflick, 1974). Still, this phenomenon also exists *in vivo*, and the altered phenotype of senescent cells in proliferative tissues is believed to cause age-associated dysfunctions (Campisi, 1998). In skin, for instance, dermal thinning and collagen breakdown may be due to increasing amounts of senescent fibroblasts, which overexpress collagenase and underexpress collagenase inhibitors (West et al., 1989).

The involvement of replicative senescence in skin aging is further suggested by the observation of parallel changes in specific biomarkers in aged skin and in senescent keratinocytes. Thus, senescence-associated β -galactosidase is overexpressed in epidermis from old donors (Dimri et al., 1995); telomere shortening, observed in senescent keratinocytes (Matsui et al., 2000), is responsible for cutaneous symptoms of normal and pathological aging (Boukamp, 2005; Hofer et al., 2005); functional binding of epidermal growth factor (EGF) is poorly efficient in senescent keratinocytes (Shi and Isseroff, 2005) as in aged epidermis (Reenstra et al., 1996); oxidative stress is associated with both cellular

senescence and skin aging (Hu et al., 2000; Kohen and Gati, 2000; Petropoulos et al., 2000); in aged skin as in senescent keratinocytes, the stress-activated MAP-kinase pathway is increased, thereby up-regulating c-Jun and matrix metalloproteinases (MMPs) (Chung et al., 2000; Kang et al., 2003). Up-regulation of inflammatory cytokines and activation of the inflammation-prone transcription factor NF- κ B, which are hallmarks of the aging condition (Chung et al., 2006) and possible causes of extrinsic skin aging (Thornfeldt, 2008), also occur in senescent keratinocytes *in vitro* (Bernard et al., 2004; Perera et al., 2006). Therefore skin aging and keratinocyte senescence, although they are distinct phenomena, are obviously in close relationship.

This view is further suggested by the fact that in Werner syndrome (WS), many of the tissues showing premature aging are those which remain proliferative during adult life, and cell cultures from WS patients indeed display a reduced replicative lifespan *in vitro*. Hence Werner syndrome may be considered, at least in part, as a syndrome of accelerated cellular senescence (Davis et al., 2007).

In this work, we have addressed the characters of cellular senescence in epidermal keratinocytes. Previous reports have stated that senescent keratinocytes are irregular-shaped, enlarged and flattened, with clear vacuoles in perinuclear cytoplasm (Kang et al., 2000; Rheinwald et al., 2002). Electron microscopy data shows

* Corresponding author. Tel.: +972 2658 5051; fax: +972 2658 5428.

E-mail address: milner@vms.huji.ac.il (Y. Milner).

an enlargement of cytoplasm but not of nucleus, an increase in number and size of perinuclear vacuoles, and an overall decrease in cellular organelle density. After an initial period of exponential growth in culture, an increasing fraction of cells stop DNA synthesis and display higher β -galactosidase activity. Upon completion of the proliferation step in most cells, terminal differentiation occurs with the expression of cytokeratins 1 and 10 (Kang et al., 2000). A close relationship exists between senescence and apoptosis, which both can be induced by oxidative stress and DNA damage, and are controlled by p53 (Vogelstein et al., 2000). Although UV-induced, p53-dependent apoptosis is inhibited by replicative senescence (Chaturvedi et al., 1999), p53-independent, cell surface receptor-activated apoptosis is exacerbated in senescent cells and aged tissues (DeJesus et al., 2002; Wang et al., 2004).

Using light and electron microscopy, fluorometry, flow cytometry and immunoblotting, we defined a panel of biomarkers of senescence and aging in the epidermal tissue. We examined the effects of Dead Sea minerals (DSM), which are known to reduce skin inflammatory disorders like psoriasis (Hodak et al., 2003, 2004), on these biomarkers. We showed that DSM can limit the progression of senescent characters in aging cells, and provide a protection against UV-induced apoptosis. Such a multifactorial evaluation of cell aging, and of the effects of protective agents, makes possible an efficient and sensible evaluation of anti-aging agents through marker profiling.

2. Materials and methods

2.1. Materials

2.1.1. Culture media

For keratinocytes from primary cultures: KGM-2 Bulletkit (Clonetics CC-3107); for HaCaT: DME-F12 medium completed with 2 mM glutamine, 5% fetal bovine serum and an antibiotic–antifungal mixture (Biological Industries, Kibbutz Beit Haemek, Israel).

2.1.2. Antibodies

Mouse monoclonal anti-P21 (sc-817), rabbit polyclonal anti-Bcl 2 (sc-492) and anti- β tubulin (sc-9104) from Santa Cruz; rabbit monoclonal anti-Ki67 (RM-9106), mouse monoclonal anti- β galactosidase (MS1329) from NeoMarkers; mouse monoclonals anti-P53 (R7154), anti-cytokeratin 10 (M7002) from Dako; mouse monoclonal anti-P16 (K0077-3) from MBL-Clinisciences; mouse monoclonal anti-involucrin from Sigma (I 9018); rabbit polyclonal anti-“Advanced Glycation Products” (mainly carboxymethyllysine) were a gift from Dr. Hilaire Bakala.

2.2. Skin cell and organ cultures

2.2.1. Keratinocyte primary cultures

Keratinocyte primary cultures were derived from infant foreskins or adult breast reductions, and processed as previously described (Brégère et al., 2003).

2.2.2. Organ cultures

Skin samples were obtained from healthy donors undergoing plastic surgery, cut into 3 × 3 mm pieces, and incubated in culture plates on a stainless steel grid, dermis immersed in DME-F12 medium with 5% fetal bovine serum and antibiotic–antifungal mixture. For immunodetection experiments, samples were fixed with 4% paraformaldehyde in phosphate buffered saline (PBS) and sectioned. Alternatively they were trypsinized, and keratinocytes were suspended in PBS and analyzed by flow cytometry. All experiments performed with organ cultures have been repeated with skin from at least three independent donors.

2.3. Electron microscopy

Keratinocytes were cultivated on 0.5 × 0.5 cm polycarbonate slides, washed in PBS, and fixed *in situ* 1 h at room temperature with 4% paraformamide, 2.5% glutaraldehyde, 0.2 M cacodylate buffer (pH 7.4). They were stained with 1% OsO₄/1.5% potassium ferricyanide in 0.2 M cacodylate buffer, gradually dehydrated by ethanol, and submitted to epon infiltration as described (Feinstein et al., 1998). Polymerization was allowed to proceed for 48 h at 60 °C, and ultrathin sections were cut using a LKB Ultratome III. Pictures were captured on a Technai-12 electron microscope equipped with a MegaView II CCD camera. For each passage, 6 different cultures and 24 different samples were processed and analyzed.

2.4. Measurements of keratinocyte fluorescence

Keratinocytes were suspended by trypsin, washed and resuspended in PBS. Cell suspensions were analyzed in a Perkin-Elmer LS 50B fluorescence reader. To obtain differential spectra, the two profiles were normalized for optimal coincidence, and then compared. These experiments have been repeated using keratinocyte cultures from at least three independent primary isolates.

2.5. Flow cytometric analysis

2.5.1. Cell suspensions

Keratinocytes were detached from culture plates by trypsin digestion and resuspended in PBS at a density of 10⁶ cells/ml. Suspensions were analyzed in a Becton Dickinson flow cytometer with 488 nm incident wavelength.

2.5.2. Autofluorescence analysis

The cell suspensions were analyzed directly for emission at 560 nm.

2.5.3. Total protein content determination

Cells were fixed in two steps: (1) 15 min incubation in PBS, 3% paraformaldehyde (PFA), at 30 °C; (2) addition of two volumes of methanol and incubation for 1 h at 4 °C. After two washes in PBS, 5 × 10⁵ cells were resuspended in 400 μ l of PBS, 0.1 μ M fluorescein iso-thio-cyanate (FITC), and incubated 1 h at 30 °C. Cells were washed in PBS and analyzed at 530 nm emission wavelength.

2.5.4. Immunodetection of cellular proteins

Cell suspensions were fixed in 2% PFA, 15 min at 30 °C, and fixed in methanol as above. After two washes in PBS, 5 × 10⁵ cells were resuspended in 400 μ l of PBS containing a specific antibody, 2 h at 30 °C. Cells were washed again in PBS and incubated with a FITC-conjugated, secondary antibody, 1 h at 30 °C. Cells were washed, resuspended in PBS, and analyzed at 488 nm/530 nm.

2.5.5. Intracellular β -galactosidase assay

Intracellular β -galactosidase assay was adapted from Fiering et al. (1991). Fifty microlitre of a keratinocyte suspension in PBS at 10⁷ cells/ml were pre-warmed at 37 °C, and mixed with 50 μ l of pre-warmed, 2 mM fluorescein di- β galactoside (FDG). After 2 min at 37 °C, the reaction was stopped with 0.5 ml of ice-cold PBS, and cells were analyzed at 488 nm/530 nm excitation/emission wavelengths.

2.6. Cell adherence assay (adapted from Goldman and Bar-Shavit, 1979)

Cells grown in multi-well culture plates were washed in PBS, fixed with 3% PFA 10 min at room temperature, washed with 0.01 M borate buffer (pH 8.5) 5 min at 37 °C, and stained with 1%

methylene blue in the same conditions. Excess dye was removed by three washes in 0.01 M borate buffer. Remaining, fixed dye was extracted by 0.1 N HCl, 20 min at 37 °C, and measured by absorption spectrophotometry at 590 nm.

2.7. Thymidine incorporation assay

Pieces of human skin (0.5 × 0.5 cm) were incubated 20 h at 37 °C in Dulbecco's modified Eagle's medium (DMEM) with 4 µCi/ml of [methyl-³H] thymidine. Medium was removed, and samples were washed with 5 mM thymidine in PBS. Skin was heated 2 min at 65 °C in PBS; the epidermal sheet was separated from the dermis, and washed in 70% methanol containing 5 mM thymidine. Epidermal samples were weighted, and [methyl-³H] thymidine incorporation was measured by scintillation counting.

2.8. Measurements of mitochondrial activity

2.8.1. Keratinocyte cultures

Cells were grown in 24-well plates to about 200,000 cells/well, washed with PBS, and incubated 1 h at 37 °C in PBS with 0.5 mg/ml 3-(4,5-dimethylthiazol-2-yl)-2,5-diphenyltetrazolium bromide (MTT; Calbiochem # 475989). Substrate was removed by PBS washes, and cells were incubated in isopropanol 30 min at room temperature with shaking, to dissolve formazan crystals thoroughly. Optical densities of supernatants were read at 570 nm in 96-well plates, and normalized to the actual number of cells estimated by methylene blue staining.

2.8.2. Organ cultures

Skin samples were washed with PBS, heated for 1 min at 56 °C, and the epidermis was peeled off. Epidermis fragments were weighted, transferred into sterile wells containing 200 µl of 0.5 mg/ml MTT in PBS, and incubated 1 h at 37 °C. Following operations were performed as above.

2.9. Immunoblots

2.9.1. Western blots

Cells scraped from culture plates, or skin fragments, were boiled 5 min in 0.25 M Tris-HCl pH 6.8, 5% glycerol, 5% β-mercaptoethanol, 1% sodium dodecyl sulphate (SDS), and processed as previously described (Wang et al., 2004). Densitometric evaluations were performed using the Image Gauge program.

2.9.2. Dot blots

Skin samples from punch biopsies were processed as above, and protein contents were estimated by staining 3 µl samples with Coomassie blue on Whatman 3MM paper, in parallel with a bovine serum albumin (BSA) scale. Then 1 µg samples were deposited in quadruplicate on a 3MM filter, heat-dried, washed with PBS and stained with Ponceau red to check protein amounts using the Image Gauge program. The filter was washed in PBS and incubated in blocking buffer (10% milk, 0.2% Tween 20 in PBS) 1 h at room temperature, then with a specific antibody overnight at 4 °C in the same buffer. Following operations were performed as above. Specific immunoreactivities were calculated for each dot.

3. Results

3.1. Morphology of senescent human keratinocyte

Human keratinocytes from primary cultures were cultivated in Clonetics KGM-2 defined medium at low Ca²⁺ concentration. In these conditions, lifespan was found limited to 22 population dou-

blings (PDs) on average, independently of donor age, as reported by Kang et al. (2000). After initial plating of epidermal cells, a proliferation-proficient population attached to the plate and began to divide. The actual size of this population could vary between experiments, and the number of PDs during this primary growth was not known. In subsequent passages, cells were collected at 80% confluence, and seeding density was chosen so as to obtain 3 PDs at early passages (1–2), and 2 PDs at late passages (4–5), when plating efficiency and growth rate were reduced.

At early passages, relatively homogenous monolayers of small (10–20 µm in diameter) polygonal cells were observed, whereas at late passages, cells became irregular in size and in shape, finally reaching up to 50 µm in diameter (Fig. 1a). The enlargement of senescent cells in culture was accompanied by differentiation, leaving dead cells on the top of the culture (arrows). Other cells with apoptotic aspect swelled out and detached from the plate (not shown), as expected from previous evidence from our lab and from others, that the apoptotic pathway is activated in senescent keratinocytes (Min et al., 1999; Wang et al., 2004).

Morphological changes were also illustrated by flow-cytometric analysis of keratinocyte populations. Flow cytometric diagrams (light scattering) show that in young cultures, 95% of the cells remained in sector I (low scattering values), while with serial passages, a massive shift is observed toward elevated values of forward and side scattering, corresponding to major changes in cell shape, and in cytoplasmic optical properties (Fig. 1b). The percentages of dots mapping within the oval marker of the figure progressively increase from 6 to 20% of the total cell number, and visibly underestimate the actual proportion of cells with altered scattering properties.

Ultrastructural changes in cells between early and late passages were examined by electron microscopy. Fig. 1c shows a keratinocyte at first passage (P1), where a large spheric nucleus displays a nucleolus (nl) surrounded by homogenous chromatin, and is enveloped by a regular membrane (nm). The cytoplasm contains highly dense mitochondria (mt) with classical divisions of internal *cristea* (crests). Some cellular vacuoles, containing dispersed granules, may be lysosomes (ly) harboring protein complexes and occasional aggregates. Keratin fibers were not seen, as expected since proliferating keratinocytes cultivated in low calcium, serum-free medium display few features of differentiation, and a less developed tonofilament system (Pillai et al., 1988).

From the third passage (P3) and onward (Fig. 1d), cell populations become more heterogenous, displaying enlarged cytoplasm with ultrastructural alterations. Although nuclei do not change in size, they have irregular shapes and are often split. Organelles are concentrated in the perinuclear zone, virtually absent from distal portions of the cytoplasm. Mitochondrial density in most cases increases with the passages, and structural alterations are clearly visible. The cytoplasm of senescent cells can display different aspects, like local increase of organelle concentrations, continuous fields of keratin tonofilaments extending from the nucleus to the plasma membrane, or large areas devoid of organelles.

The nature of the organelles appearing in aged cells is shown by EM at higher magnification. Fig. 2a–d shows different aspects of early senescence in the perinuclear cytoplasm of P3 cells. In Fig. 2a, crests are seen distributed regularly in most mitochondria (“mt”) although not in parallel mode, and some organelles are seen devoid of typical crests. Piles of membranes that look like Golgi sacks (“go”) are also visible, as well as relatively empty lysosome-like vacuoles (“ly”). In Fig. 2b, one can see mitochondrial crests irregularly distributed in longitudinal sections, sometimes lacking in semi-transversal sections (“**”). Dotted membranes are still seen in the cells at this stage, indicating rough reticulum (“rr”). Only rare, nascent fibers (likely keratin tonofilaments) are present in some places (“kf”). In Fig. 2c, regular mitochondrial structures are seen alternating with swelled portions without crests. In Fig. 2d, long-

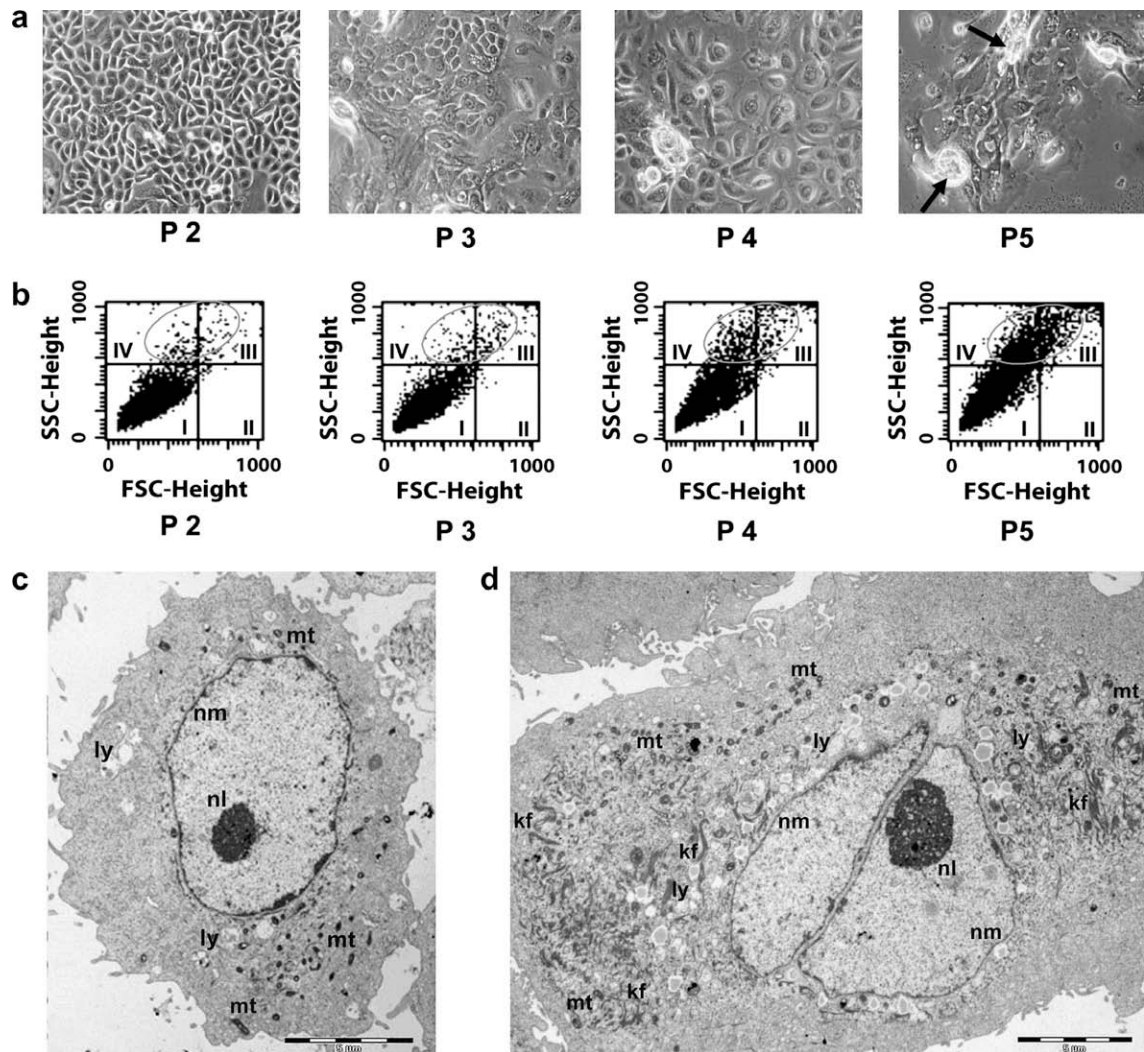


Fig. 1. Microscopic and flow-cytometric characterization of senescent phenotype in human keratinocytes. (a) Human keratinocytes derived from primary cultures were cultivated by serial passaging in low-calcium medium, and passages 2–5 were analyzed in parallel by phase-contrast microscopy and flow cytometry. (b) Flow-cytometric analysis of successive passages: the abundance of dots in upper sectors (III and IV) correspond to larger, phenotypically senescent cells with higher cytoplasmic granularity; as an indication of the progressive shift of aging cells to this senescent phenotype, the proportion of dots mapping within the oval marker increased from 6% at P2 and P3 to 12% at P4, and 20% at P5. **SSC**, side scattering; **FSC**, forward scattering. (c and d) EM views of human keratinocytes grown in low-calcium, serum-free medium, at P2 and P4, respectively. kf, keratine fibers; ly, lysosome-like vacuole; mt, mitochondria; nl, nucleolus; nm, nuclear membrane. Magnification 4000 \times .

shaped, less dense mitochondria are seen, and the enrichment in keratin bundles is apparent, consistently with previous data showing induction of keratin expression upon growth arrest in low calcium medium (Kang et al., 2000). Fig. 2e–f represents an advanced senescent stage of P4 cells. In Fig. 2e, representing aged cells at passage 5, irregular mitochondrial patterns are seen, as well as lysosome-like vesicles (“ly”) filled up with unidentified, dense, granules, possibly lipofuscin (Brunk and Terman, 2002). Fig. 2f clearly shows advanced alteration of mitochondrial structures and thinning of the nuclear membrane (“nm”).

3.2. Age-associated changes in skin fluorescence

It was shown by Stamatas et al. (2006) that skin fluorescence changes go together with aging: a decrease at 295/340 nm (excitation/emission, respectively), contributed mainly by tryptophan, is associated with cell proliferation; increases at 340/390 nm and 360/420 nm are associated with collagen cross-links, and an increase at 375/500 nm is associated with elastin cross-links. Here, it can be seen from the excitation spectrum shown in Fig. 3a that

295/340 nm fluorescence in keratinocyte cultures decreases in late, compared with early, passages. Therefore we conclude that autofluorescence may be a valid marker for both skin aging *in vivo* and cellular senescence *in vitro*.

Lipofuscin is an insoluble, final product of protein oxidation composed of denatured polypeptides bound to oxidized lipids, that accumulates as deposits in lysosomes of aging tissues (Brunk and Terman, 2002) and strongly fluoresces at 600–620 nm (Sparrow and Boulton, 2005). When keratinocyte suspensions from late and early passages were compared, we indeed observed a fluorescence increase at 480/620 nm in senescent cultures, as shown in the emission spectrum of Fig. 3b. This indication of lipofuscin accumulation fits nicely with the EM data above, which display dense electron-opaque material accumulating in lysosome-like vacuoles of senescent keratinocytes (Fig. 2e).

3.3. Flow-cytometric analysis of epidermal senescence

We submitted keratinocyte cultures to flow-cytometric analysis at early (P1–P2) or late (P4–P5) passages, using different labeling

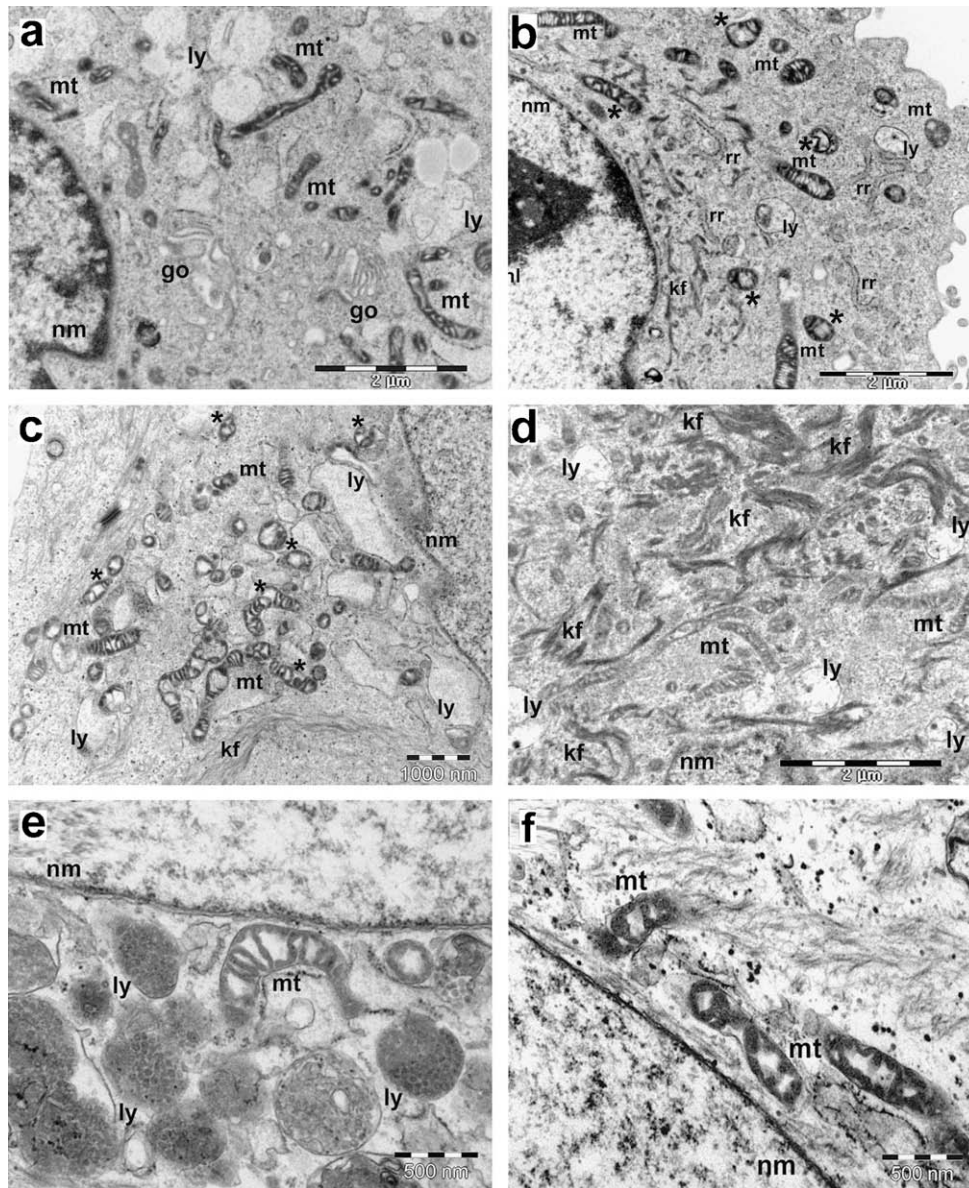


Fig. 2. Ultrastructural changes in aging keratinocytes. EM views of human keratinocytes cultures in low calcium, KGM-2 Bulletkit medium, taken at P3 (a–d) and P4 (e–f). go, Golgi apparatus; kf, keratine fibers; ly, lysosome-like vacuole; mt, mitochondria; *, irregular mitochondrial patterns; nl, nucleolus; nm, nuclear membrane; rr, rough endoplasmic reticulum. Magnifications: (a), 14,000 \times ; (b and c), 12,000 \times ; (d), 15,000 \times ; (e and f), 30,000 \times .

methods. An overall increase of autofluorescence at 488/560 nm appeared with passaging, that followed a bimodal distribution profile in the cell population (Fig. 4 top, left panels). This is consistent with the increase observed in direct fluorescence at 480/620 nm, and likely to correspond to lipofuscin accumulation. A bimodal pattern was observed in senescent cultures also with the proliferation marker Ki67, detected by quantitative immunolabeling. An overall decrease in Ki67 was observed, in a context where total protein amounts per cell increased (Fig. 4 bottom, center and left panels). Thus, a subpopulation of senescent cells, rich in lipofuscin and poor in Ki67, seems to develop at late passages, while other cells retain a seemingly normal (i.e. non-senescent) phenotype. Asymmetrical flow cytograms were also generated for total protein contents (non-specifically labelled with FITC), or with “advanced glycosylated endproducts” (AGEs), reflecting the oxidative modification of proteins by glycation adducts (Petropoulos et al., 2000). The distribution modes followed by these markers reveal a large heterogeneity of keratinocyte populations at late passages, reflect-

ing the actual variability of the senescent phenotype in these cells. By contrast, the replicative senescence marker p16 displayed a 2.5-fold increase while keeping a monomodal distribution in late passages, thus showing that it varies to the same extent in all kinds of senescing cells. Some epidermal samples of different ages were obtained from surgery, dissociated by trypsin and analyzed by flow cytometry. Age-associated changes were found in senescence biomarkers, consistently with those observed in keratinocyte cultures (data not shown).

Fas receptor is known to increase in amounts in aged keratinocytes, while the relevant apoptotic pathway is upregulated (Wang et al., 2004). Here, flow cytometric results showed a global increase in Fas receptor at late passages, with a complex distribution corresponding to phenotype variability. The senescence marker p16 was increased with passages and fitted a monomodal distribution, apparently being a good indicator of replicative age, rather than labeling a senescent subpopulation (Fig. 4 top, center panels).

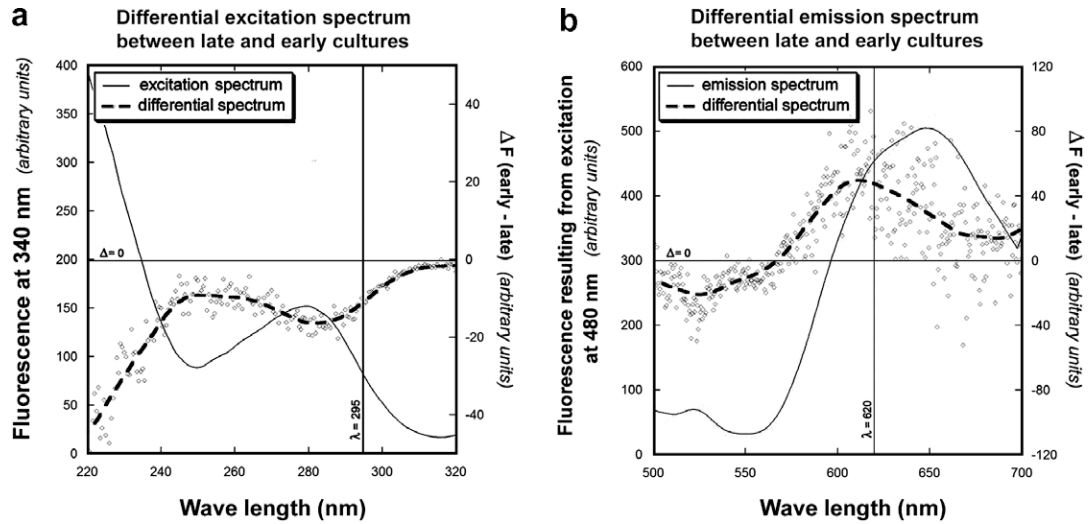


Fig. 3. Senescence-associated changes in keratinocyte autofluorescence. Fluorescence spectra were measured in parallel in suspensions of late (P5) and intermediate-early (P3) keratinocytes. (a) Excitation spectrum, emission set up at 340 nm; (b) emission spectrum, excitation set up at 480 nm. Differential spectra between late and early appear in dashed lines. Maximum absorption of tryptophan (295 nm), and maximum emission of lipofuscin (620 nm), are marked by vertical lines. ΔF (early-late), difference in fluorescence measured between late- and early-passage cells (normalized).

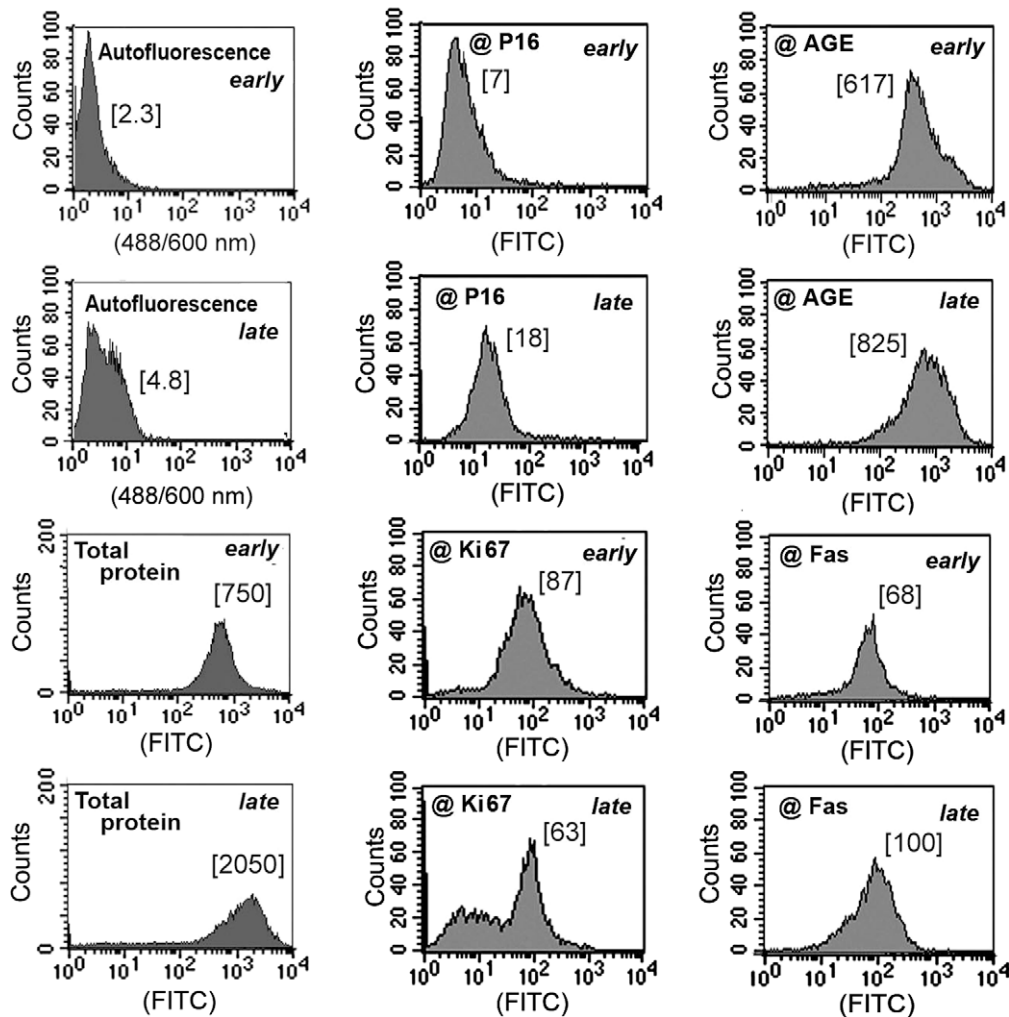


Fig. 4. Biomarkers of senescence in epidermal cells. Cell suspensions were obtained and processed from keratinocyte cultures as described in the Methods section. Flow cytograms represent fluorescent signals resulting from autofluorescence, non-specific FITC binding in cells (total protein contents), or FITC-conjugated antibody binding to specific antigens, as marked in each window. Numbers between square brackets correspond to average fluorescence in the overall cell population normalized to 10,000 cells. “Early” and “late” correspond to P2 and P4 cultures, respectively.

3.4. Effects of Dead Sea minerals on epidermal cell viability and senescence

Bathing in Dead Sea was known to be beneficial for skin by improving skin barrier function, increasing stratum corneum hydration, reducing skin roughness and inflammation (Proksch et al., 2005), and dramatically reducing the inflammation in psoriasis (Hodak et al., 2004). Because all these processes are, at various extents, relevant to the aged condition of skin, we addressed the effects of mild osmotic stress induced by DSM preparations in keratinocyte cultures.

Dilutions of “Osmoter”, a commercial preparation of DSM (Table 1), were tested for toxicity on HaCaT cells, a spontaneously immortalized line of human keratinocytes that retained the ability to differentiate *in vitro* (Boukamp et al., 1988). Osmoter was added to the growth medium of dividing or confluent cultures for 48 h; dead cells spontaneously detached from the plate, and adherent, living cells were stained with methylene blue. Fig. 5a shows that viability and proliferation were minutely affected by Osmoter at concentrations lower than 0.5% (v/v). The LD₅₀ of Osmoter on HaCaT cells was reached with an effective concentration of 1%, which corresponds approximately to a 0.15 N (i.e. 2-fold) increase of osmolarity in the culture medium. Osmoter effects on cell death and proliferation were found similar in HaCaT cells and in normal human keratinocytes (not shown). At subtoxic doses, Osmoter was found to increase mitochondrial activity monitored by MTT assay, and cell proliferation measured by thymidine incorporation (Fig. 5a).

When similar experiments were performed in skin organ cultures, these two “vitality” parameters were even further stimulated. Western blots revealed that the levels of Ki67 were increased, and those of p16 consistently decreased. Surprisingly, β-galactosidase activity was not significantly altered by this treatment of the skin (Fig. 5b).

3.5. Effects of Dead Sea minerals on senescence markers in keratinocyte cultures

For further investigation of DSM effects on the senescent phenotype, we analyzed Osmoter-induced changes in senescence markers in intermediate (P3) and in late (P5) keratinocyte cultures. After a 48-h incubation, cellular extracts were prepared and analyzed by SDS-PAGE and Western blotting. In the absence of treatment, senescing P5 keratinocytes displayed an increase in p16 and involucrin expression, and a decrease in apoptosis inhibitor Bcl 2,

when compared with less senescent, P3 cells. Osmoter treatment produced little change in P3 cells, but in P5 cultures, enriched in senescent cells, it notably reduced p16 and involucrin signals, and increased Bcl 2, so that these three markers “returned” to their values in non-senescent cells (Fig. 6a). These effects were maximized at a dilution of 0.25% (v/v), corresponding to an increase in medium osmolarity by 0.037 N (approximately +25%). We conclude that, at least in keratinocyte cultures, DSM can modulate senescence markers, and hence may curb cellular aging.

3.6. Effects of Dead Sea minerals on senescence markers in skin

A similar analysis was applied to human skin *in vivo*: 2% Osmoter, formulated in water/oil emulsion, and void emulsion as a placebo control, were applied on the inner fore-arms of 10 volunteers of both sexes and various ages (from 24 to 48 yr, average 37 yr), twice a day for 4 weeks. Then skin samples were collected by punch biopsies, analyzed by dot immunoblots, and specific signals were quantified by densitometry. It can be seen in Fig. 6b that p16 decreased significantly, like it did in keratinocyte cultures. p21, another marker of senescence pertaining to the p53-dependent pathway, also tended to decrease, albeit slightly. Interestingly, Fas receptor was increased, indicating that the extrinsic apoptotic pathway may be stimulated by Osmoter. β-galactosidase did not show a significant change, like in cell cultures.

3.7. Interference of Dead Sea minerals with UVB-induced apoptosis

Moderate sun exposure can induce stress response and premature aging, while higher doses induce apoptosis and sunburn cells (Yaar and Gilchrist, 2001). We investigated UVB-induced apoptotic cells by flow cytometry, in HaCaT keratinocytes (Boukamp et al., 1988), using double fluorescent labeling by FITC-conjugated annexin V and propidium iodide. Indeed, apoptotic cells were accumulating in irradiated cultures (see circles in Fig. 7a). We observed also that apoptosis takes place a few hours after UVB exposure and further develops for 20 h after irradiation (not shown). Fig. 7b summarizes a series of experiments in which cells were submitted to different UVB doses, and demonstrates that a 48-h pretreatment by Osmoter curbs down the number of apoptotic cells in a dose-dependent manner. This shows that DSM can exert a protective effect against UV-induced damage in keratinocytes, consistent with their effect on aging biomarkers in cultured keratinocytes and in skin.

4. Discussion

Increasing frequencies of senescent cells are a hallmark of aging in mammalian tissues, in particular in human skin (Dimri et al., 1995). Consistently, biomarkers of replicative senescence are associated with *in vivo* aging, as stated above. Therefore we have addressed the senescent phenotype of epidermal keratinocytes as means to evaluate skin biological aging, and its control by active compounds.

4.1. Complexity of the senescent phenotype in epidermal cells

As early as on second passage, cultured keratinocytes begin to increase in size, and to diversify into subpopulations displaying senescent and differentiated characters. Senescent cells display dramatic changes in cytoplasm size and perinuclear organelle contents. Some sectors of the cytoplasm are entirely filled with tonofilaments, presumably keratin, in agreement with previous observations that oral keratinocytes differentiate in low-calcium

Table 1
Composition of “Mineral Skin Osmoter”

	Salt normality (N)		Salt normality (N)
Na	0.118 (2.720 g/l)	Rb	3.5×10^{-6} ($<3 \times 10^{-4}$ g/l)
K	0.054 (2.100 g/l)	Sb	$<1.6 \times 10^{-7}$ ($<2 \times 10^{-5}$ g/l)
Ca	0.873 (35.000 g/l)	Sr	7.6×10^{-3} (0.670 g/l)
Mg	3.815 (92.700 g/l)	V	$<7.9 \times 10^{-5}$ (<0.004 g/l)
Ba	6.6×10^{-5} (0.009 g/l)	Th	$<8.6 \times 10^{-8}$ ($<2 \times 10^{-5}$ g/l)
Cd	$<1.8 \times 10^{-7}$ ($<2 \times 10^{-5}$ g/l)	U	$<8.4 \times 10^{-8}$ ($<2 \times 10^{-5}$ g/l)
Co	$<3.4 \times 10^{-5}$ (<0.002 g/l)	Zn	$<3.06 \times 10^{-5}$ (<0.002 g/l)
Cu	$<3.15 \times 10^{-5}$ (<0.004 g/l)	Cl	<u>9.75</u> (346 g/l)
Cr	$<3.85 \times 10^{-4}$ (<0.02 g/l)	Br	<u>0.175</u> (14 g/l)
Fe	$<3.58 \times 10^{-5}$ (<0.002 g/l)	B	0.011 (0.120 g/l)
Li	5.76×10^{-3} (0.040 g/l)	As	2.7×10^{-5} (0.002 g/l)
Mn	1.82×10^{-4} (0.010 g/l)	I	6.30×10^{-7} (8×10^{-8} g/l)
Mo	$<1.04 \times 10^{-6}$ ($<10^{-4}$ g/l)	SiO ₂	$<3.33 \times 10^{-4}$ (<0.02 g/l)
Ni	$<3.4 \times 10^{-5}$ (<0.002 g/l)	SiO ₄	$<2.2 \times 10^{-3}$ (<0.2 g/l)
Pb	$<9.6 \times 10^{-8}$ ($<2 \times 10^{-5}$ g/l)		

Underlined: major constituents.

Source: Geological Survey – Ministry of National Infrastructures, State of Israel, especially for Ahava-Dead Sea Laboratories.

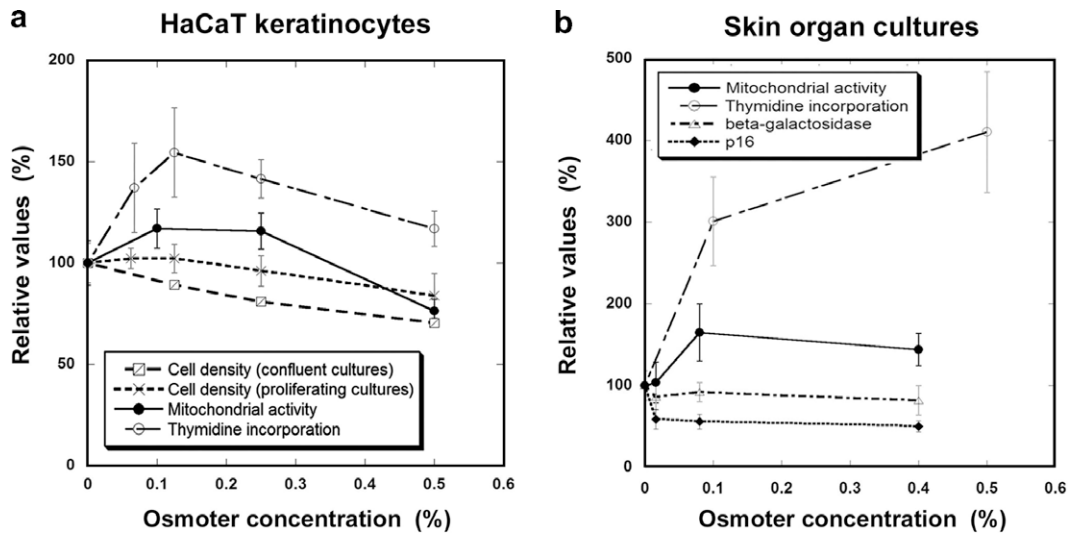


Fig. 5. Effects of Dead Sea minerals on cell survival and proliferation, mitochondrial activity and senescence biomarker p16. HaCaT line keratinocytes (a), and skin organ cultures (b), were incubated 48 h with Osmoter on culture plates. Densities of adherent (living) cells were determined by methylene blue; mitochondrial activities were measured *in situ* by MTT oxidation; [methyl-³H] thymidine incorporation in DNA and its measurement were performed as described in Section 2.7; β -galactosidase and p16 were monitored by Western blotting and immunoreactivity, followed by densitometry. “Relative values” refer to untreated controls as 100%.

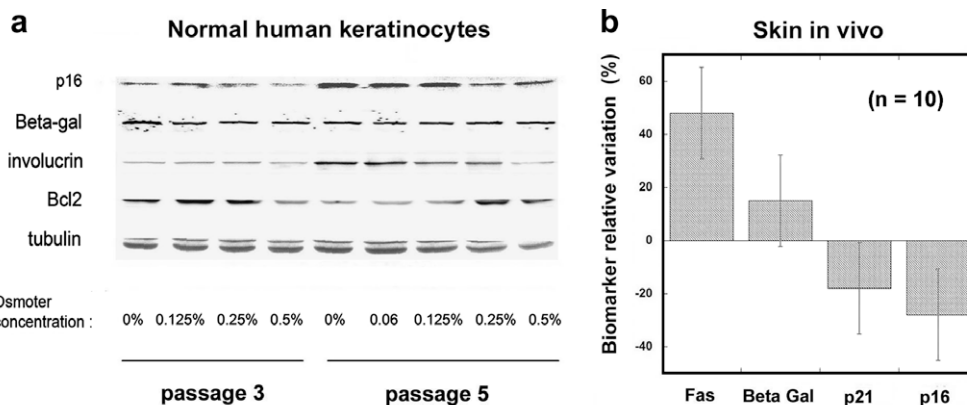


Fig. 6. Effects of Dead Sea minerals on senescence biomarkers in keratinocyte cultures and skin *in vivo*. (a) Keratinocyte cultures at passages 3 and 5 were incubated 48 h with Osmoter, harvested and lysed in sample buffer. Extracts were analyzed by SDS-PAGE and Western immunoblotting. (b) Two percent Osmoter in water–oil emulsion, and void emulsion as a control, were applied twice a day on the inner forearms of 10 donors, for 4 weeks. Punch biopsies were taken (2×4 mm) and extracted in 1% SDS as described in Section 2.9. Then biomarkers were assayed in the extracts by dot immunoblots, and their relative abundance measured by densitometry. Variations observed between treated and untreated skin areas are plotted in a bar diagram.

growth medium upon senescent growth arrest (Kang et al., 2000). Other sectors show large, transparent vacuoles like in apoptotic cells (Min et al., 1999). Others accumulate lysosome-like vacuoles filled with granules, likely proteolysis-resistant bodies and lipofuscin (see below).

Senescent features have also been characterized at biophysical and biochemical levels. Thus, 295/340 nm autofluorescence was found to decrease at late passages in keratinocyte cultures, as it does in aging skin *in vivo* (Stamatas et al., 2006). This further suggests that replicative senescence is linked to aging state. At 480/620 nm, the fluorescent signal increased with passages, probably reflecting lipofuscin accumulation. Therefore, direct fluorometry can be used to evaluate the senescent status of epidermal cells *in vitro*, and of aging skin *in vivo*. If fluorescent parameters can be correlated with specific pathways of biological aging, they might provide a basis for a non-invasive and safe evaluation of aging characteristics in skin *in situ*.

Lipofuscin accumulation was also assessed by flow cytometry: in late-passage keratinocytes, 488/560 nm fluorescence increased

and followed a bimodal distribution, indicating the presence of at least two distinct phenotypes in senescent cultures. This fits with the observation that senescent and non-senescent cells indeed co-exist in keratinocyte populations (Kang et al., 2000; Rheinwald et al., 2002). We found quantitative changes and bimodal or asymmetrical distribution also for other markers like AGEs, total protein content, Fas receptor, and Ki67, reflecting a phenotype heterogeneity for these markers in senescent cultures. Only p16 kept a monomodal distribution after a 2.5-fold increase, thereby exhibiting features of an indicator of replicative age (see Fig. 4).

Table 2 summarizes the results contributed by our laboratory to describe the aged keratinocyte phenotype. As a whole, it comes out that a variety of pathways are associated with keratinocyte senescence and skin aging, among which cell cycle and proliferation, protein metabolism, lysosomal enzymes, apoptosis, differentiation and hormone signaling. All these pathways co-operate to define the senescent phenotype of skin cells and tissue as a multi-factorial, multi-functional phenomenon, and a biological basis of functional changes in aged skin.

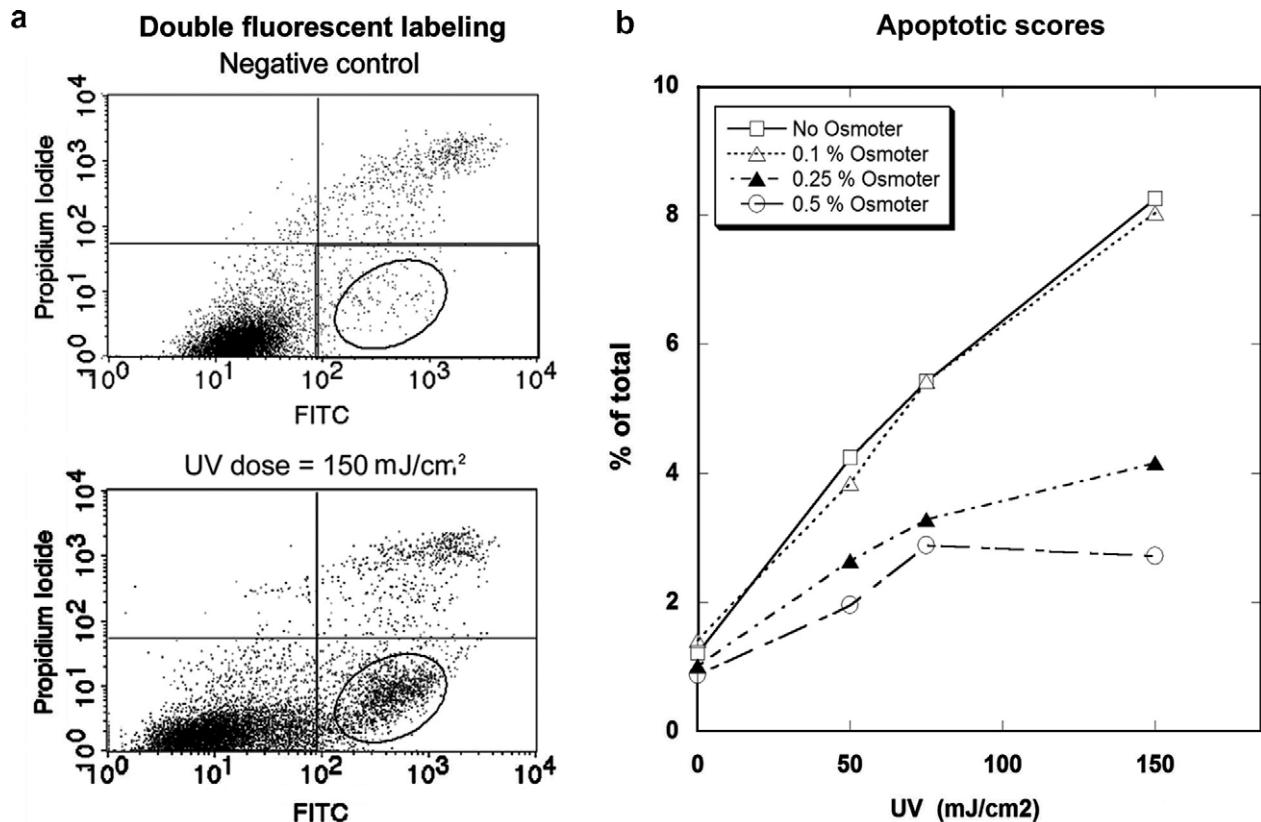


Fig. 7. DSM effects on UV-induced apoptosis in keratinocyte cultures. HaCaT cultures were exposed to UV doses of 50–200 mJ/cm², double-labeled with FITC-conjugated annexin V (green fluorescence) and propidium iodide (PI, red fluorescence), and analyzed by flow cytometry as previously described (Wang et al., 2004). (a) Fluorescent signals were dot-plotted according to the intensities of green (annexin V) versus red (PI) fluorescence, so as to define different cell populations in different areas: viable cells (low annexin V, low PI), apoptotic cells (high annexin V, low PI, marked with a circle) and dead cells (high annexin V, high PI); occurrence of apoptosis in UV-irradiated cells is immediately visible by comparison of the two plots. (b) Cells were pre-incubated 48 h with Osmoter, and the proportions of apoptotic cells were plotted versus UV doses, using different salt concentrations (see inset).

4.2. Comprehensive approach of senescence and biological aging in epidermis

The multifunctional character of senescence and aging in skin cells and tissue has been addressed previously by transcriptome analysis, using the cDNA microarray methodology (Kang et al., 2003; Yoon et al., 2004; Lener et al., 2006; Perera et al., 2006). All these experiments indeed provided evidence for the occurrence of multiple changes in gene expression related to cell growth, apoptosis, transcription factors, cytokines, extracellular matrix proteins and more, thereby establishing the multifaceted nature of cellular senescence and skin aging.

Although transcriptome data have a rich informative content, the actual aged condition depends directly on expressed proteins and their activities, and only indirectly on gene transcription. Therefore, a phenotypic profile of skin aging should be deduced essentially from protein analysis, and include markers of replicative senescence, oxidative stress, protein modification, inflammatory cytokine secretion, apoptosis, differentiation, and more. Interestingly, some of these biomarkers may be optionally associated with senescence and aging and define keratinocyte subpopulations, or types of aging skin, with specific trends. As an example, functions involved in circadian rhythms have been described as variable aging markers in humans some years ago (Duffy and Feuers, 1991). And indeed, pathways like oxidative stress response, apoptosis, selective proteolysis, inflammatory response or differentiation can contribute to senescence to variable extents, depending on individual parameters and conditions. Accordingly, a multifunc-

tional approach of the senescent phenotype can address the issue of biological variability, too often ignored in molecular analysis of functions and diseases.

4.3. Multifunctional assessment of drug efficacy: the case of Dead Sea minerals

Adapting therapeutic strategies to biological diversity would bring a major breakthrough in current medicine, as stated for cardiovascular (Siest et al., 2005) and anticancer drugs (Garcia-Foncillas et al., 2006). For each pathology, a set of relevant biomarkers can be defined, and used to test the effects of each possible drug in an experimental model. Then, systematic analysis of these markers in each patient can help to define the best therapeutic fitting between drug action and patient profile. In such an approach of skin aging control, we have checked the effects of DSM on a set of senescence-associated protein markers.

We found that proliferation and survival of keratinocyte cultures were significantly decreased by Osmoter only at concentrations above 0.5%, corresponding to salt concentrations of 19 mM Mg²⁺, 4.4 mM Ca²⁺, 0.6 mM Na⁺, 0.038 mM Sr²⁺, 0.029 mM Li⁺, and to a 50% increase in overall salt concentration in the culture medium. This contrasts with an earlier report, stating that proliferation of dermal fibroblasts in culture was inhibited by two components of DSM, MgCl₂ and MgBr₂ (Levi-Schaffer et al., 1996). In that work, however, each salt was applied separately, at concentrations (50 and 75 mM) that can be reached with Osmoter only under conditions of toxicity. Remarkably, it was found that Osmoter restored

Table 2
Biomarker variations in aging epidermal cells

Increase factors for:	Cell cultures		Skin extracts
	Flow cytometry	Extracts	
Protein/cell (FITC, Bradford)	2.0 ± 0.7 ^a	4.7 ± 2.6 ^c	–
Autofluorescence (488/530 nm)	1.5 ± 0.3 ^a	–	–
Autofluorescence (488/560 nm)	1.9 ± 0.4 ^a	–	–
Ki 67 (IR)	0.65 ± 0.15 ^a	–	–
β-Galactosidase (activ)	2.5 ± 1.0 ^a	2.8 ± 0.7 ^b	3.8 ± 0.5 ^b
Caspase 1 (activ)	–	–	1.8 ± 1.0 ^d
Caspase 3 (activ)	–	–	1.8 ± 1.0 ^d
20S proteasome (IR)	–	0.53 ± 0.2 ^b	0.41 ± 0.2 ^b
Carbonyls (Oxyblots)	–	~1.8 ^b	~3 ^b
HNE adducts (IR)	–	~6.2 ^b	~8 ^b
p16 (IR)	2.3 ± 0.7 ^a	~2.3 ^a	–
Fas R (IR)	1.8 ± 0.5 ^{a,d}	~5.1 ^d	~3.8 ^d
Fas L (IR)	–	–	~8 ^{d,f}
FADD (IR)	–	–	~4.5 ^d
Bcl2 (IR)	0.47 ± 0.7 ^{a,d}	0.5 ± 0.15 ^{a,d}	0.15 ± 0.05 ^d
Involucrin (IR)	0.95 ± 0.25 ^a	~2.8 ^a	–
Estrogen receptor (IR)	–	1.4 ^e	3.2 ^e
Sumo (IR)	–	0.4 ^e	0.5 ^e
Cell size (Microscopy)	3 ± 1.5 ^a	–	–

Keratinocytes were compared between early (1–2) and late (4–5) culture passages, and skin between young (less than 40 years) and old (more than 50 years) individuals. For each kind of measurement, old-versus-young ratios are given. Standard deviation was calculated for flow cytometric, ELISA and colorimetric assays. Densitometric evaluations of band intensity in Western blots are presented with an approximation symbol. Values derived from microarray data by computational analysis stand in italic. activ, enzymatic activity; FITC, non-specific FITC labeling; IR, immunoreactivity.

^a This work.

^b Petropoulos et al. (2000).

^c Brégégère et al. (2003).

^d Wang et al. (2004).

^e Ma'or and Milner, unpublished.

^f Assayed in membranal and microsomal pellets.

in aged cells the marker levels found in young cells, promoting the expression of p16 and involucrin, and reducing that of Bcl-2. Immunoblots also revealed a decrease in p16 in Osmoter-treated skin *in vivo*, and a similar trend in p21. An interesting possibility would be that Osmoter rejuvenates the keratinocyte population by eliminating poorly proliferative, differentiation-prone cells, rather than changing the phenotypic expression in all cells. This is not suggested by our results, however, since the *in vitro* effects of Osmoter on keratinocyte cultures have been measured in a low-calcium growth medium that prevents differentiation until senescent growth arrest (Kang et al., 2000).

Osmoter dramatically reduced the number of apoptotic cells following exposure to UVB in keratinocyte cultures. Yet, topical application of Osmoter increased the expression of Fas, the head of a death receptor pathway of apoptosis (Nagata, 1999) upregulated in senescent keratinocytes (Wang et al., 2004). This recalls the overexpression of Fas in senescent keratinocytes and dermal fibroblasts, which are sensitized to death receptor-mediated apoptosis (DeJesus et al., 2002; Wang et al., 2004) although they are resistant to “intrinsic” apoptosis (Wang, 1995; Qin et al., 2002). Fas expression is turned off in actinic keratosis and carcinomas (Filipowicz et al., 2002), suggesting that Fas may antagonize tumoral proliferation in senescent keratinocytes. Therefore DSM, which reduces the expression of several senescence markers and enhances Fas receptor, may altogether antagonize the aging process and help to limit pathogenic proliferation, as already established for psoriasis.

Acknowledgements

We thank Ms. Naomi Feinstein for expert assistance and counseling in electron microscopy. This work was funded by the Dead Sea and Arava Science Center, Ministry of Science, State of Israel

and by the European co-operative research project “CELLAGE”, CRAF-1999-71628.

References

- Bernard, D., Gosselin, K., Monte, D., Vercamer, C., Bouali, F., Pourtier, A., Vanderbunder, B., Abbadie, C., 2004. Involvement of Rel/nuclear factor-κB transcription factors in keratinocyte senescence. *Cancer Res.* 64, 472–481.
- Boukamp, P., Petrussevska, R.T., Breitkreuz, D., Hornung, J., Markham, A., Fusenig, N.E., 1988. Normal keratinization in a spontaneously immortalized aneuploid human keratinocyte cell line. *J. Cell Biol.* 106, 761–771.
- Boukamp, P., 2005. Skin aging: a role for telomerase and telomere dynamics? *Curr. Mol. Med.* 5, 171–177.
- Brégégère, F., Soroka, Y., Bismuth, J., Friguet, B., Milner, Y., 2003. Cellular senescence in human keratinocytes: unchanged proteolytic capacity and increased protein load. *Exp. Gerontol.* 38, 619–629.
- Brunk, U.T., Terman, A., 2002. Lipofuscin: mechanisms of age-related accumulation and influence on cell function. *Free Radic. Biol. Med.* 33, 611–619.
- Campisi, J., 1998. The role of cellular senescence in skin aging. *J. Invest. Dermatol. Symp. Proc.* 3, 1–5.
- Chaturvedi, V., Qin, J.Z., Denning, M.F., Choubey, D., Diaz, M.O., Nickoloff, B.J., 1999. Apoptosis in proliferating, senescent, and immortalized keratinocytes. *J. Biol. Chem.* 274, 23358–23367.
- Chung, J.H., Kang, S., Varani, J., Lin, J., Fisher, G.J., Voorhees, J.J., 2000. Decreased extracellular-signal-regulated kinase and increased stress-activated MAP kinase activities in aged human skin *in vivo*. *J. Invest. Dermatol.* 114, 177–182.
- Chung, H.Y., Sung, B., Jung, K.J., Zou, Y., Yu, B.P., 2006. The molecular inflammatory process in aging. *Antioxid. Redox Signal.* 8, 572–582.
- Davis, T., Wyllie, F.S., Rokicki, M.J., Bagley, M.C., Kipling, D., 2007. The role of cellular senescence in Werner syndrome – Toward therapeutic intervention in human premature aging. *Ann. NY Acad. Sci.* 1100, 455–469.
- DeJesus, V., Rios, I., Davis, C., Chen, Y., Calhoun, D., Zakeri, Z., Hubbard, K., 2002. Induction of apoptosis in human replicative senescent fibroblasts. *Exp. Cell Res.* 274, 92–99.
- Dimri, G.P., Lee, X., Basile, G., Acosta, M., Scott, G., Roskelley, C., Medrano, E.E., Linskens, M., Rubeli, I., Pereira-Smith, O., Peacocke, M., Campisi, J., 1995. A biomarker that identifies senescent human cells in culture and in aging skin *in vivo*. *Proc. Natl. Acad. Sci. USA* 92, 9363–9367.
- Duffy, P.H., Feuers, R.J., 1991. Biomarkers of aging: changes in circadian rhythms related to the modulation of metabolic output. *Biomed. Environ. Sci.* 4, 182–191.
- Feinstein, N., Parnas, D., Parnas, H., Dudel, J., Parnas, I., 1998. Functional and immuno-cytochemical identification of glutamate autoreceptors of an NMDA type in crayfish neuromuscular junction. *J. Neurophysiol.* 80, 2893–2899.
- Fiering, S.N., Roederer, M., Nolan, G.P., Mickle, D.R., Parks, D.R., Herzenberg, L.A., 1991. Improved FACS-Gal: flow-cytometric analysis and sorting of viable eukaryotic cells expressing reporter gene constructs. *Cytometry* 12, 291–301.
- Filipowicz, E., Adegboyega, P., Sanchez, R.L., Gatalica, Z., 2002. Expression of CD95 (Fas) in sun-exposed human skin and cutaneous carcinomas. *Cancer* 94, 814–819.
- Garcia-Foncillas, J., Bandrés, E., Zárate, R., Ramirez, N., 2006. Proteomic analysis in cancer research: potential application in clinical use. *Clin. Transl. Oncol.* 8, 250–261.
- Goldman, R., Bar-Shavit, Z., 1979. Dual effect of normal and stimulated macrophages and their conditioned media on target cell proliferation. *J. Natl. Cancer Inst.* 63, 1009–1016.
- Hayflick, L., 1974. The longevity of cultured human cells. *J. Am. Geriatr. Soc.* 22, 1–12.
- Hodak, E., Gottlieb, A.B., Segal, T., Politi, Y., Maron, L., Sukes, J., David, M., 2003. Climatotherapy at the Dead Sea is a remittive therapy for psoriasis: combined effects of epidermal and immunologic activation. *J. Am. Dermatol.* 49, 451–457.
- Hodak, E., Gottlieb, A.B., Segal, T., Maron, L., Lotem, M., Feinmesser, M., David, M., 2004. An open trial of climatotherapy at the Dead Sea for patch-stage mycosis fungoides. *J. Am. Acad. Dermatol.* 51, 33–38.
- Hofer, A.C., Tran, A.C., Aziz, O.Z., Wright, W., Novelli, G., Shay, J., Lewis, M., 2005. Shared phenotypes among segmental progeroid syndromes suggest underlying pathways of aging. *J. Gerontol. A Biol. Sci. Med. Sci.* 60, 10–20.
- Hu, H.L., Forsey, R.J., Blades, T.J., Barratt, M.E.J., Parmar, P., Powell, J.R., 2000. Antioxidants may contribute in the fight against ageing: *in vitro* model. *Mech. Ageing Dev.* 121, 217–230.
- Kang, M.K., Bibb, C., Baluda, M.A., Rey, O., Park, N.H., 2000. *In vitro* replication and differentiation of normal human oral keratinocytes. *Exp. Cell Res.* 258, 288–297.
- Kang, M.K., Kameta, A., Shin, K.H., Baluda, M.A., Kim, H.R., Park, N.H., 2003. Senescence-associated genes in normal human oral keratinocytes. *Exp. Cell Res.* 287, 272–281.
- Kohen, R., Gati, I., 2000. Skin low molecular weight antioxidants and their role in aging and in oxidative stress. *Toxicology* 148, 149–157.
- Lener, T., Moll, P.R., Rinnerthaler, M., Bauer, J., Aberger, F., Richter, K., 2006. Expression profiling of aging in the human skin. *Exp. Gerontol.* 41, 387–397.
- Levi-Schaffer, F., Shani, J., Politi, Y., Rubinchik, E., Brenner, S., 1996. Inhibition of proliferation of psoriatic and healthy fibroblasts in cell culture by selected Dead Sea salts. *Pharmacology* 52, 321–328.
- Matsui, M., Miyasaka, J., Hamada, K., Ogawa, Y., Hiramoto, M., Fujimori, R., Aioi, A., 2000. Influence of aging and cell senescence on telomerase activity in keratinocytes. *J. Dermatol. Sci.* 22, 80–87.

- Min, B.M., Woo, K.M., Lee, G., Park, N.H., 1999. Terminal differentiation of normal human oral keratinocytes is associated with enhanced cellular TGF- β and phospholipase C- γ 1 levels and apoptotic cell death. *Exp. Cell Res.* 249, 377–385.
- Nagata, S., 1999. Fas ligand-induced apoptosis. *Ann. Rev. Genet.* 33, 29–55.
- Perera, R.J., Koo, S., Bennett, C.F., Dean, N.M., Gupta, N., Qin, J.Z., Nickoloff, B.J., 2006. Defining the transcriptome of accelerated and replicatively senescent keratinocytes reveals links to differentiation, interferon signaling, and notch related pathways. *J. Cell. Biochem.* 98, 394–408.
- Petropoulos, I., Conconi, M., Wang, X., Hoemel, B., Brégégère, F., Milner, Y., Friguet, B., 2000. Increase of oxidatively modified proteins is associated with a decrease of proteasome activity and content in aging cells. *J. Gerontol.* 55A, B220–B227.
- Pillai, S., Bikle, D.D., Hincebergs, M., Elias, P.M., 1988. Biochemical and morphological characterization of growth and differentiation of normal human neonatal keratinocytes in a serum-free medium. *J. Cell. Physiol.* 134, 229–237.
- Proksch, E., Nissen, H.P., Bremgartner, M., Urquhart, C., 2005. Bathing in a magnesium-rich Dead Sea salt solution improves skin barrier function, enhances skin hydration, and reduces inflammation in atopic dry skin. *Int. J. Dermatol.* 44, 151–157.
- Qin, J.Z., Chaturvedi, V., Denning, M.F., et al., 2002. Regulation of apoptosis by p53 in UV-irradiated human epidermis, psoriatic plaques and senescent keratinocytes. *Oncogene* 21, 2991–3002.
- Reenstra, W.R., Yaar, M., Gilchrist, B.A., 1996. Aging affects epidermal growth factor receptor phosphorylation and traffic kinetics. *Exp. Cell Res.* 227, 252–255.
- Rheinwald, J.G., Hahn, W.C., Ramsey, M.R., Wu, J.Y., Guo, Z., Tsao, H., De Luca, M., Catricalà, C., O'Toole, K.M., 2002. A two-stage, p16^{INK4a}- and p53-dependent keratinocyte senescence mechanism that limits replicative potential of telomere status. *Mol. Cell. Biol.* 22, 5157–5172.
- Shi, B., Isseroff, R.R., 2005. Epidermal growth factor (EGF)-mediated DNA-binding activity of AP-1 is attenuated in senescent human epidermal keratinocytes. *Exp. Dermatol.* 14, 519–527.
- Siest, G., Marteau, J.B., Maumus, S., Berrahmoune, H., Jeannesson, E., Samara, A., Batt, A.M., Visvikis-Siest, S., 2005. Pharmacogenomics and cardiovascular drugs: need for integrated biological system with phenotypes and proteomic markers. *Eur. J. Pharmacol.* 527, 1–22.
- Sparrow, J.R., Boulton, M., 2005. RPE lipofuscin and its role in retinal pathobiology. *Exp. Eye Res.* 80, 595–606.
- Stamatas, G.N., Estanislao, R.B., Suero, M., Rivera, Z.S., Li, J., Khaiat, A., Kollias, N., 2006. Facial skin fluorescence as a marker of the skin's response to chronic environmental insults and its dependence on age. *Br. J. Dermatol.* 154, 125–132.
- Thornfeldt, C.R., 2008. Chronic inflammation is etiology of extrinsic aging. *J. Cosmet. Dermatol.* 7, 78–82.
- Vogelstein, B., Lane, D., Levine, A.J., 2000. Surfing the p53 network. *Nature* 408, 307–310.
- Wang, E., 1995. Senescent human fibroblasts resist programmed cell death, and failure to suppress Bcl2 is involved. *Cancer Res.* 55, 2284–2292.
- Wang, X., Brégégère, F., Soroka, Y., Kayat, A., Redziniak, G., Milner, Y., 2004. Enhancement of Fas-mediated apoptosis in ageing human keratinocytes. *Mech. Ageing Dev.* 2004 (125), 237–249.
- West, M.D., Pereira-Smith, O.M., Smith, J.R., 1989. Replicative senescence of human skin fibroblasts correlates with a loss of regulation and expression of collagenase activity. *Exp. Cell Res.* 184, 138–147.
- Yaar, M., Gilchrist, B., 2001. Ageing and photoageing of keratinocytes and melanocytes. *Clin. Exp. Dermatol.* 26, 583–591.
- Yoon, I.K., Kim, H.K., Kim, Y.K., Song, I.H., Kim, W., Kim, S., Baek, S.W., Kim, J.H., Kim, J.R., 2004. Exploration of replicative senescence-associated genes in human dermal fibroblasts by cDNA microarray technology. *Exp. Gerontol.* 39, 1369–1378.